Hindawi Publishing Corporation
Mathematical Problems in Engineering
Volume 2012, Article ID 670761, 12 pages
doi:10.1155/2012/670761

Research Article

Multifractals Properties on the Near Infrared Spectroscopy of Human Brain Hemodynamic

Truong Quang Dang Khoa and Vo Van Toi

Biomedical Engineering Department, International University of Vietnam National Universities, Block 6, Linh Trung Ward, Thu Duc District, Ho Chi Minh City, Vietnam

Correspondence should be addressed to Truong Quang Dang Khoa, khoa@ieee.org

Received 7 October 2011; Accepted 4 December 2011

Academic Editor: Carlo Cattani

Nonlinear physics presents us with a perplexing variety of complicated fractal objects and strange sets. Naturally one wishes to characterize the objects and describe the events occurring on them. Moreover, most time series found in "real-life" applications appear quite noisy. Therefore, at almost every point in time, they cannot be approximated either by the Taylor series or by the Fourier series of just a few terms. Many experimental time series have fractal features and display singular behavior, the so-called singularities. The multifractal spectrum quantifies the degree of fractals in the processes generating the time series. A novel definition is proposed called full-width Hölder exponents that indicate maximum expansion of multifractal spectrum. The obtained results have demonstrated the multifractal structure of near-infrared spectroscopy time series and the evidence for brain imagery activities.

1. Introduction

Neurophysiological and neuroimaging technologies have contributed much to our understanding of normative brain function. Functional magnetic resonance imaging (fMRI) is currently considered the "gold standard" for measuring functional brain activation. The limitations of fMRI include the requirement that participants must lie within the confines of the magnet bore, which limits its use for many applications. The readout gradients in the imaging pulse sequences also produce a loud noise [1]. fMRI is also highly sensitive to movement artifact; subject movements on the order of a few millimeters can invalidate the data. And fMRI systems are quite expensive [2].

In recent years, functional near-infrared spectroscopy (NIRS) has been introduced as a new neuroimaging modality with which to conduct functional brain-imaging studies. NIRS technology uses specific wavelengths of light, introduced at the scalp, to enable

the noninvasive measurement of changes in the relative ratios of deoxygenated hemoglobin and oxygenated hemoglobin during brain activity. A wireless NIRS system consists of personal digital assistant software controlling the sensor circuitry, reading, saving, and sending the data via a wireless network. This technology allows the design of portable, safe, affordable, noninvasive, and minimally intrusive monitoring systems [3].

For such advanced features, NIRS signal processing really becomes an attractive field for computational science. Izzetoglu et al. investigated the canceling of motion artifact noise from NIRS signals by Wiener filter [4]. Izzetoglu et al. presented a statistical analysis of NIRS signals for the purpose of cognitive state assessment while the user performs a complex task [5]. The results indicated that the rate of change in the blood oxygenation of NIRS signals was significantly sensitive to task load changes and correlated fairly well with performance variables. Fantini et al. describe a specific frequency-domain instrument for near-infrared tissue spectroscopy. It has been proven that the hemodynamic changes monitored with NIR spectroscopy correlate with the activation state of the cortex in response to a stimulus [6, 7]. Sitaram et al. presented the results of signal analysis indicating that distinct patterns of hemodynamic responses exist that could be utilized in a pattern classifier [8].

Although there are many computing analyses on NIRS biomedical signals, there is not yet any work mentioning the aspects of NIRS physics. This paper continuously explores physical aspects of NIRS following a paper mentioned about nonlinear characteristics [9]. In this paper, we report an evidence for multifractality in biomedical NIRS signals and furthermore detect that the singularities indicate the state changes of brain activities. Since the conception of multifractal structure was first reported in 1986 by Halsey et al. [10], an approach based on wavelets transform was developed latter by Muzy et al. [11] and Mallat [12] called wavelet transform modulus maxima (WTMM). This theory has been greatly developed and applied in many study fields especially in biomedical researches. In 1999, Ivanov et al. [13] reported in Nature that multifractality is endogenous in healthy heartbeat dynamics both in awake and sleep states and thus does not depend on external factors such as levels of physical activities. In 2001, Amaral et al. [14] found the multifractal complexity of cardiac dynamics decreased or markedly lost when blocking the sympathetic or parasympathetic branch of the neuron autonomic system. Ohashi et al. [15] generalized WTMM in order to analyze positive and negative changes separately and show different singularity spectra depending on the direction of changes in human heartbeat interval data during sympathetic blockade, time series of daytime human physical activity of healthy individuals and daily stock price records. Shimizu et al. [16] investigated WTMM on functional magnetic resonance imaging (fMRI) time series to extract local singularity exponents to identify activated areas in human brain. In 2007, Yang et al. [17] distinguished among healthy people and heart diseased once by multifractal singularity spectrum area of synchronous 12-lead electrocardiogram (ECG) signals.

Although there are a lot of papers on the multifractality of the biological signals, there are few studies that clarify the reason of multifractal and the relation between the multifractality and biological functions.

During the last decades, a number of authors have claimed not only correlations between memory span and mental speed but also with electrophysiological and hemoglobin variables of brain waves. In [18], H. Weiss and V. Weiss determined the information entropy of working memory capacity. The congruence between multiples of memory span and multiples of a fundamental brain wave was the first important discovery. Relationships between different frequencies correspond to mechanisms designed to minimize interference, couple activity via stable phase interactions, and control the amplitude of one frequency

relative to the phase of another. These mechanisms are proposed to form a framework for spectral information processing [19]. In addition, we discovered the relationship between brain waves in motor imaging activities measured by NIRS and chaos properties in [20]. Furthermore, in this paper, we investigated WTMM to detect the singularities on NIRS time series. The obtained results indicate the task periods of brain activities. Furthermore, the parameters of WTMM models indicate physiological conditions in order to recognize left and right motor imagery tasks of human brain.

2. Methods

2.1. Wavelet Transform Modulus Maxima Method

2.1.1. Fractal Function

Self-affine functions are ones that are similar to themselves when transformed by anisotropic dilations. If $f(x)$ is a self-affine function, then $\forall x_0 \in \Re$, $\exists H \in \Re$ such that, for any $\lambda > 0$,

$$f(x_0 + \lambda x) - f(x_0) \approx \lambda^H \big(f(x_0 + x) - f(x_0)\big). \tag{2.1}$$

H is called the Hurst exponent. If $H < 1$, then f is not differentiable and the smaller H is the more singular f. Thus, H indicates the global irregularity or roughness of f. The fractal dimension of graph f is defined:

$$D_F = H - 2. \tag{2.2}$$

Fractal functions can possess multiaffine properties so that their roughness or the irregularity can fluctuate from point to point. Thus, the definition of the Hurst regularity becomes a local quantity of the velocity increment $\delta f(x_0 + l)$ around x_0 in the limit of inertial separation $l \to 0$:

$$f(x_0 + l) - f(x_0) \sim l^{h(x_0)}. \tag{2.3}$$

The local the Hurst exponent $h(x)$ is also called the Hölder exponent of f at point x. This is primarily related with the strength of the singularity of f at this point.

At any given point x_0, the Hölder exponent is given by the largest exponent such that there exists a polynomial $P_n(x - x_0)$ of order $n < h(x_0)$ and a constant $C > 0$, so that, for any point x in the neighborhood of x_0, the following relation holds.

$$\big|f(x) - P_n(x - x_0)\big| \leq C|x - x_0|^h. \tag{2.4}$$

$h(x_0)$ measures how irregular f is at x_0. The higher the exponent $h(x_0)$, the more regular the function f.

In a signal with fractal features, an immediate question one faces is "how to quantify the fractal properties of such a signal?" The first problem is to find the set of locations of the singularities $\{x_i\}$ and to estimate the value of h for each x_i.

2.1.2. Using Wavelets Transform (WT) to Detect Singularities

WT is a space-scale analysis which consists in expanding signals in terms of wavelets which are constructed from a single function, the mother wavelet ψ, by means of translation and dilation. The WT of a real-valued function f is defined as

$$T_\psi[f](x_0, a) = \frac{1}{a}\int_{-\infty}^{+\infty} f(x)\psi\left(\frac{x - x_0}{a}\right)dx, \tag{2.5}$$

x_0 is the space parameter; a (>0) is the scale parameter.

The analyzing wavelet is usually well localized in both space and frequency. An interesting property of the wavelet transform is that the coefficients at these maxima are enough to encode the information contained in the signal. These maxima are defined, at each scale a, as the local maxima of $|T_\psi[f](x, a)|$. Moreover, as one follows a maxima line from the lowest scale to higher and higher scales, one is following the same singularity. This fact allows for the calculation of h_i by a power law fit to the coefficients of the wavelet transform along the maxima line.

The first possibility is that we find a single value $h_i = H$ for all singularities; the signal is then said to be monofractal. The second, more complex, possibility is that we find several distinct values for h; the signal is then said to be multifractal.

2.1.3. Wavelet Transform Modulus Maxima Method (WTMM)

The term modulus maxima describes any point (x_0, a_0) such that $|T_\psi[f](x, a)|$ is locally maximum at $x = x_0$:

$$\frac{\partial T_\psi[f](x_0, a_0)}{\partial x} = 0. \tag{2.6}$$

This local maximum is a strict local maximum in either the right or the left neighborhood of x_0. Maxima lines are called the connected curves of local maxima in the space-scale plane (x, a) along which all points are modulus maxima.

Let $\Im(a)$ be the set of all the maxima lines that exist at the scale a which contain maxima at any scale $a' \leq a$. A partition function is defined in terms of WT coefficients:

$$Z(q, a) = \sum_{l \in \Im(a)} \left(\sup_{\substack{(x,a') \in l \\ a' \leq a}} \left| T_\psi[f](x, a') \right| \right)^q. \tag{2.7}$$

The partition function Z measures the sum at a power q of all these wavelet modulus maxima. One can define the exponent $\tau(q)$ from the power-law behavior of partition function:

$$Z(q,a) \sim a^{\tau(q)}. \tag{2.8}$$

Thus, one can estimate $h(x_0)$ as the slope of log-log plot of Z versus scale a. The singularity spectrum can be determined from the Legendre transform of the partition function scaling exponent $\tau(q)$:

$$D(h) = \min_{q}(qh - \tau(q)), \tag{2.9}$$

where $h = \partial\tau/\partial q$.

A linear $\tau(q)$ curve indicates a homogenous fractal function. A nonlinear $\tau(q)$ curve indicates a nonhomogenous function exhibiting multifractal properties; that is, the Hölder exponent $h(x)$ depends on the spatial position x.

A novel definition is proposed in this paper called full-width the Hölder exponents that indicates maximum expansion of the Hölder exponents within spectrum $D(h)$. This parameter presents better separation of different multifractal time series:

$$fwH = \delta h = h_{\max} - h_{\min}. \tag{2.10}$$

3. Biomedical Time Series Acquisition

We used a multichannel NIRS instrument, OMM-3000, from Shimadzu Corporation, Japan, to acquire oxygenated hemoglobin and deoxygenated hemoglobin concentration changes. The system operated at three different wavelengths, 780 nm, 805 nm, and 830 nm, emitting an average power of 3 mW·mm^{-2}. The illuminator and detector optodes were placed on the scalp. The detector optodes were fixed at a distance of 4 cm from the illuminator optodes. The optodes were arranged above the hemisphere on the subject's head.

Near-infrared rays leave each illuminator, pass through the skull and the brain tissue of the cortex, and are received by the detector optodes. The photomultiplier cycles through all the illuminator-detector pairings to acquire data at every sampling period. The data were digitized by the 16-bit analog-to-digital converter. Because oxygenated and deoxygenated hemoglobin types have characteristic optical properties in the visible and near-infrared light range, the change in concentration of these molecules during neurovascular coupling can be measured using optical methods. By measuring absorption changes at two (or more) wavelengths, one of which is more sensitive to Oxy-Hb and the other to Deox-Hb, changes in the relative concentrations of these chromophores can be calculated. Using these principles, researchers have demonstrated that it is possible to assess brain activity through the intact skull in adult humans.

The NIRS instrument was capable of storing the raw signals for each of the channels, one of which consists of the intensity values of 3 wavelengths, and also the derived values of oxygenated hemoglobin [Ox-Hb], deoxygenated hemoglobin [Deox-Hb], and total hemoglobin [Total-Hb] = [Ox-Hb] + [Deox-Hb] concentration changes for all time points in an output file in a prespecified format.

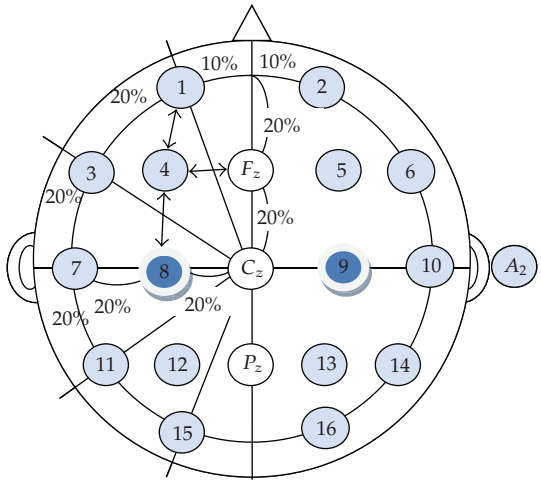

Figure 1: Measured positions based on international 10–20 system.

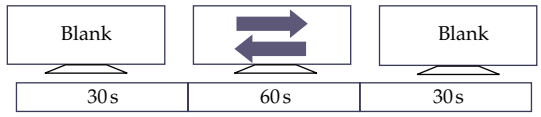

Figure 2: Experiment imagery moving tasks.

In this work, we investigate an experiment brain response on imagery moving tasks. The stimulus is a computer screen with arrows indicating left turn or right turn. The subject is a normal 30-year-old man measured during 2 mins, with the sampling time of 25 ms. In terms of optode placement, there is currently no standardized placement scheme for NIRS measurements. With such a standardized placement of electroencephalography (EEG), we have proposed 2 positions number 8 and number 9 in primary motor cortex of Brodmann's areas as shown in Figure 1 measuring left and right moving imagery tasks as shown in Figure 2.

4. Results and Discussion

This section included illustrated results in three tests, testing monofractal of fractional Brownian motion (fBM) signals, detecting singularities throughout artificial signals, and detecting singularities of real-life NIRS signals.

4.1. Testing Monofractal of Fractional Brownian Motion (fBM) Signals

Figure 3(a) displays one realization of a fractional Brownian with the Hurst exponent $H = 0.3$. The mother wavelet is chosen first derivative of Gaussian, and decomposition scale increases follow as exponent function, $a = 1.15^i$, $i = 0, \ldots, N = 35$. Figure 3(b) gives the scaling exponent $\tau(q)$, which is nearly a straight line. Fractional Brownian motions are

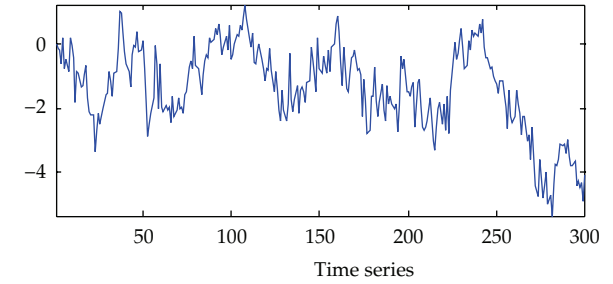

(a) Data

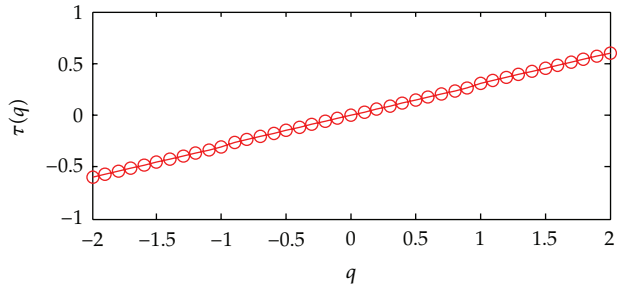

(b) Hölder exponent

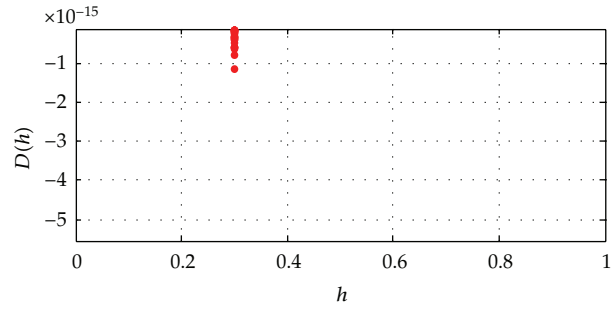

(c) Multifractal Spectrum

Figure 3: (a) A fractional Brownian with the Hurst exponent $H = 0.3$, (b) Scaling exponent $\tau(q)$ (c) Multifractal spectrum.

homogeneous fractals equal to H. The estimated spectrum in Figure 3(c) is calculated with a Legendre transform of $\tau(q)$. The theoretical spectrum $D(h)$ has therefore reduced to $\{0.3\}$.

4.2. Detecting Singularities of Multifractal Signal

Figure 4 clearly shows singularities detected by finding the abscissa where the wavelet modulus maxima is locally maximum. The mother wavelet is chosen first derivative of Gaussian, and decomposition scale increases follow as exponent function, $a = 1.15^i$, $i = 0, \ldots, N = 35$. Figure 4(a) are original data taken from illustrated example of Matlab 1-dimension continuous wavelet analysis. Figures 4(b) and 4(d) are correspondent to the chains of local maxima and wavelet coefficients $|T_\psi[f](x, a)|$ at the maximum scale. It can be found

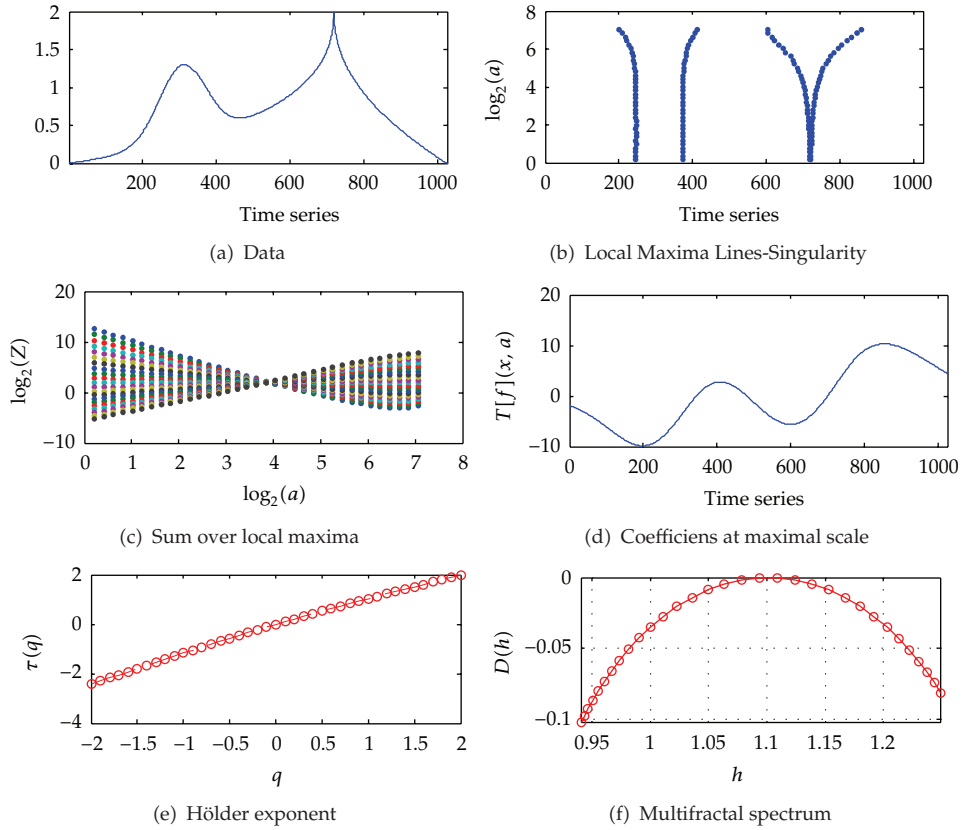

Figure 4: (a) Data testing singularities. (b) Local maxima line. (c) Partition functions. (d) Wavelet coefficients at the maximum scale. (e) Scaling exponents. (f) Multifractal spectrum.

that the beginning of chains is correspondent to local maxima of $|T_\psi[f](x,a)|$. The partition function Z measures the sum at a power $q = \{-2 : 2\}$ of all these wavelet modulus maxima shown in Figure 4(c). Figure 4(e) gives the scaling exponent $\tau(q)$, and spectrum $D(h)$ in Figure 4(f) indicates the signal is multifractal.

4.3. *Relation between Mulfractality and Biological Functions*

The objective of this paper is detection of the singularities on NIRS time series and then finding the active periods of human brain. Figures 5 and 6 are correspondent to changes in concentrations of oxyhemoglobin (Oxy-Hb) and deoxy-hemoglobin (DeOxy-Hb) using the second derivative of Gaussian, and wavelet scale increases follow as exponent function, $a = 1.15^i$, $i = 0, \ldots, N = 45$. Figure 5(b) shows all singularities, two of which reache to positive peaks of $|T_\psi[f](x,a)|$ shown in Figure 5(d) at which occur activities of brain. Concurrently Figure 6 displays two negative minima at the same positions. Only using characteristic points of interests, maxima and minima, as an extension of wavelet-based analysis of multifractal singularity, we can identify active periods of human brain. Furthermore, multifractal spectra shown in Figures 5(f) and 6(f) indicate NIRS is definitely multifractal time series. In near

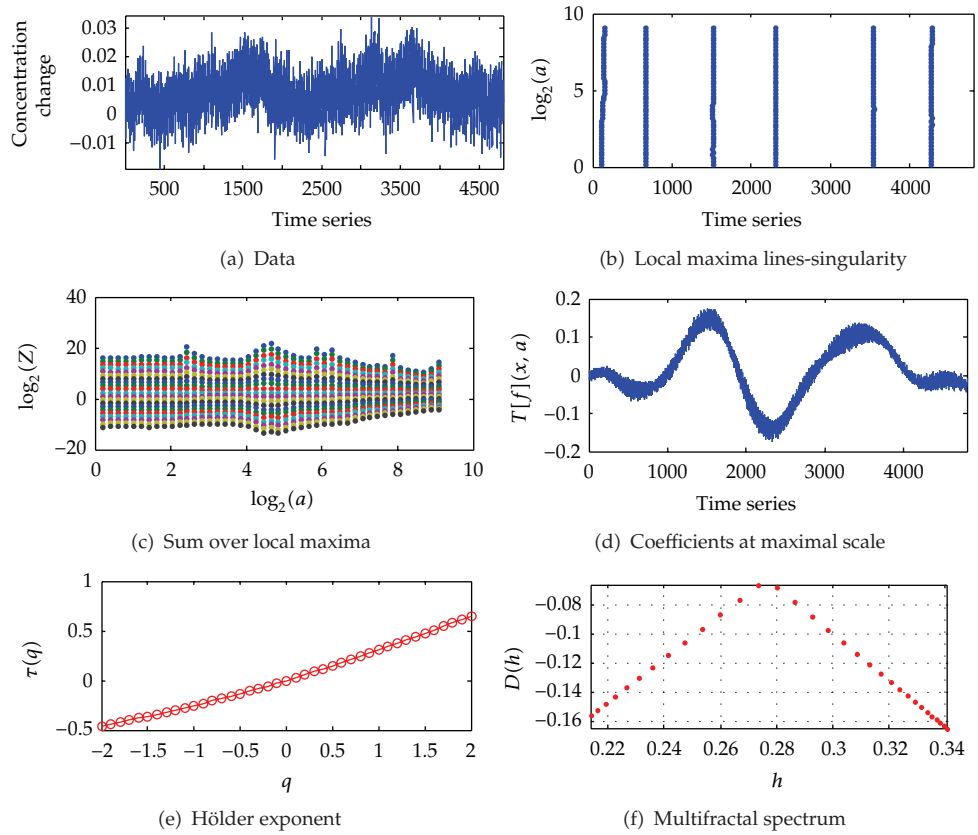

Figure 5: (a) Data of changes in concentrations of Oxy-Hb (b) Local maxima line (c) Partition functions (d) Wavelet coefficiens at the maximum scale (e) Scaling exponents (f) Multifractal spectrum.

future, we believe that the results provide greater opportunities to identify the mechanisms responsible for complex biomedical systems.

Figure 7 shows evidences that the full-width Hölder exponents are clearly different corresponding to right-hand moving tasks. The fwH in these figures is average value of three trials for the same subject. In Figure 3, while brain implement to image the right-hand task, the measurements on the right side of head at the C3 position present the wide range of Hölder exponents. This indicates that multifractal behavior of right hand, channel 1, is stronger than that of left side of brain. The notice is completely right for all three acquisition data, (Ox-Hb), (Deox-Hb) and (To-Hb). The similar results of left-hand moving imagery are shown in Figure 8. The multifractal spectrum of the left-side measurements, channel 2, indicates a wide range of the Hölder exponents.

5. Conclusions

The advantages of NIRS are well demonstrated in many recent reports, although quantification of the changes of NIRS responses is still being developed. In the present paper, we have focused mainly on detection of multifractal characteristics of NIRS time series to identify the active-state period of human brain. Multifractal parameters are regarded as a

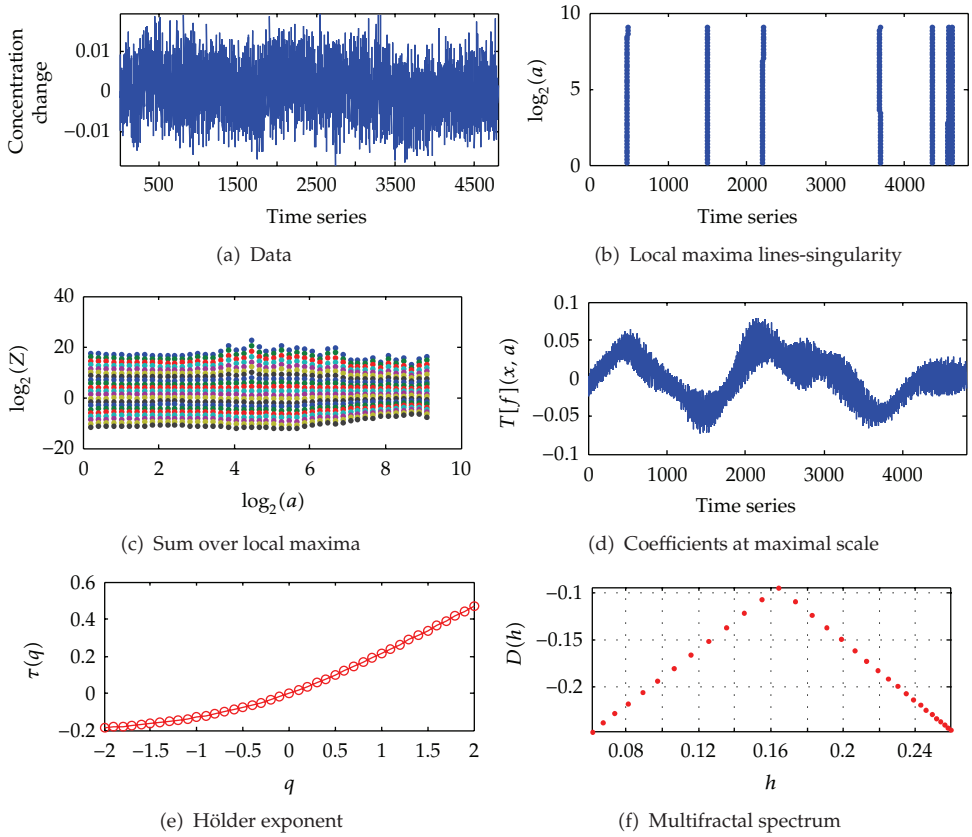

Figure 6: (a) Data of changes in concentrations of DeOxy-Hb. (b) Local maxima line. (c) Partition functions. (d) Wavelet coefficients at the maximum scale. (e) Scaling exponents. (f) Multifractal spectrum.

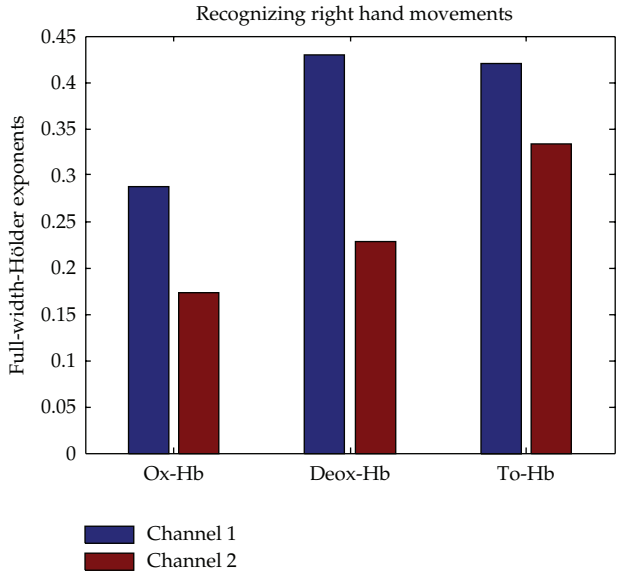

Figure 7: Average full-width Hölder exponents during right-hand motor imagery.

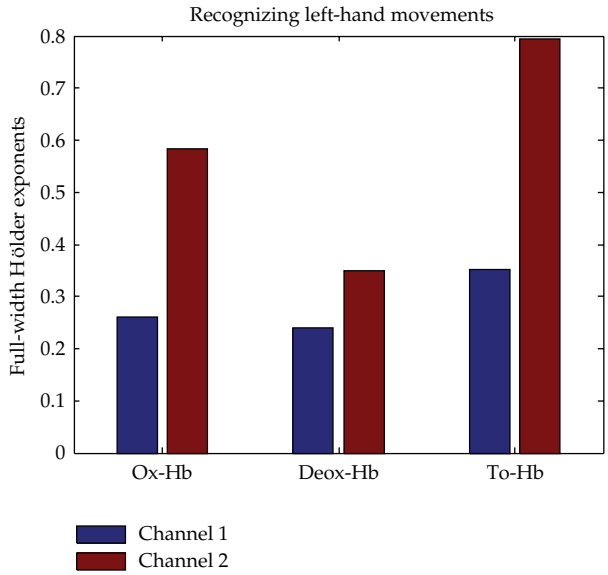

Figure 8: Average full-width-Hölder exponents during left hand motor imagery.

flexibility of human brain activities to understand brain activities. Different functional states of brain are probably governed by different degrees of multifractality. Further investigations into applications of NIRS signals could carry out meaningful contributions in medical and biological engineering.

Acknowledgements

The authors would like to acknowledge the Research Grant from the Vietnam National University in Ho Chi Minh City and the Vietnam National Foundation for Science and Technology Development (NAFOSTED) Research Grant no. 106.99-2010.11. Furthermore, They are deeply grateful for the support from our volunteers and friend.

References

[1] M. E. Ravicz, J. R. Melcher, and N. Y.-S. Kiang, "Acoustic noise during functional magnetic resonance imaging," *Journal of the Acoustical Society of America*, vol. 108, no. 4, pp. 1683–1696, 2000.

[2] S. C. Bunce, M. Izzetoglu, K. Izzetoglu, B. Onaral, and K. Pourrezaei, "Functional near-infrared spectroscopy," *IEEE Engineering in Medicine and Biology Magazine*, vol. 25, no. 4, pp. 54–62, 2006.

[3] M. Izzetoglu, K. Izzetoglu, S. Bunce et al., "Functional near-infrared neuroimaging," *IEEE Transactions on Neural Systems and Rehabilitation Engineering*, vol. 13, no. 2, pp. 153–159, 2005.

[4] M. Izzetoglu, A. Devaraj, S. Bunce, and B. Onaral, "Motion artifact cancellation in NIR spectroscopy using Wiener filtering," *IEEE Transactions on Biomedical Engineering*, vol. 52, no. 5, pp. 934–938, 2005.

[5] K. Izzetoglu, S. Bunce, B. Onaral, K. Pourrezaei, and B. Chance, "Functional optical brain imaging using near-infrared during cognitive tasks," *International Journal of Human-Computer Interaction*, vol. 17, no. 2, pp. 211–227, 2004.

[6] S. Fantini and M. A. Franceschini, "Frequency-domain techniques for tissue spectroscopy and imaging," in *Handbook of Optical Biomedical Diagnostics*, V. V. Tuchin, Ed., pp. 405–453, SPIE, Bellingham, Wash, USA, 2002.

[7] A. Sassaroli, Y. Tong, F. Fabbri, B. Frederick, P. Renshaw, and S. Fantini, "Functional mapping of the human brain with near-infrared spectroscopy in the frequency-domain," in *Lasers in Surgery: Advanced Characterization, Therapeutics, and Systems XIV*, vol. 5312 of *Proceedings of SPIE*, pp. 371–377, San Jose, Calif, USA, January 2004.

[8] R. Sitaram, H. Zhang, C. Guan et al., "Temporal classification of multichannel near-infrared spectroscopy signals of motor imagery for developing a brain-computer interface," *NeuroImage*, vol. 34, no. 4, pp. 1416–1427, 2007.

[9] T. Q. D. Khoa, H. M. Thang, and M. Nakagawa, "Testing for nonlinearity in functional near-infrared spectroscopy of brain activities by surrogate data methods," *The Journal of Physiological Sciences*, vol. 58, no. 1, pp. 47–52, 2008.

[10] T. C. Halsey, M. H. Jensen, L. P. Kadanoff, I. Procaccia, and B. I. Shraiman, "Fractal measures and their singularities: the characterization of strange sets," *Physical Review A*, vol. 33, no. 2, pp. 1141–1151, 1986.

[11] J. F. Muzy, E. Bacry, and A. Arneodo, "Multifractal formalism for fractal signals: the structure-function approach versus the wavelet-transform modulus-maxima method," *Physical Review E*, vol. 47, no. 2, pp. 875–884, 1993.

[12] S. Mallat, *A Wavelet Tour of Signal Processing*, Academic Press, 2nd edition, 1999.

[13] P. C. Ivanov, L. A. N. Amaral, A. L. Goldberger et al., "Multifractality in human heartbeat dynamics," *Nature*, vol. 399, no. 6735, pp. 461–465, 1999.

[14] L. A. N. Amaral, P. C. Ivanov, N. Aoyagi et al., "Behavioral-independent features of complex heartbeat dynamics," *Physical Review Letters*, vol. 86, no. 26, pp. 6026–6029, 2001.

[15] K. Ohashi, L. A. N. Amaral, B. H. Natelson, and Y. Yamamoto, "Asymmetrical singularities in real-world signals," *Physical Review E*, vol. 68, no. 6, Article ID 065204, 2003.

[16] Y. Shimizu, M. Barth, C. Windischberger, E. Moser, and S. Thurner, "Wavelet-based multifractal analysis of fMRI time series," *NeuroImage*, vol. 22, no. 3, pp. 1195–1202, 2004.

[17] X. Yang, X. Ning, and J. Wang, "Multifractal analysis of human synchronous 12-lead ECG signals using multiple scale factors," *Physica A*, vol. 384, no. 2, pp. 413–422, 2007.

[18] H. Weiss and V. Weiss, "The golden mean as clock cycle of brain waves," *Chaos, Solitons and Fractals*, vol. 18, no. 4, pp. 643–652, 2003.

[19] A. K. Roopun, M. A. Kramer, L. M. Carracedo et al., "Temporal Interactions between Cortical Rhythms," *Frontiers in Neuroscience*, vol. 2, no. 2, pp. 145–154, 2008.

[20] T. Q. D. Khoa, N. Yuichi, and N. Masahiro, "Recognizing brain motor imagery activities by identifying chaos properties of oxy-hemoglobin dynamics time series," *Chaos, Solitons and Fractals*, vol. 42, no. 1, pp. 422–429, 2009.